

# Canceling and inverting normal and anomalous group-velocity dispersion using space-time wave packets

Layton A. Hall<sup>1</sup> and Ayman F. Abouraddy<sup>1,\*</sup>

<sup>1</sup>CREOL, The College of Optics & Photonics, University of Central Florida, Orlando, FL 32816, USA and

\*Corresponding author: raddy@creol.ucf.edu

Angular dispersion can counterbalance normal group-velocity dispersion (GVD) that increases the wave-vector length in a dispersive medium. By tilting the wave vector, angular dispersion reduces the axial wave number in this case to match the pre-GVD value. By the same token, however, angular dispersion fails to counterbalance anomalous GVD, which in contrast reduces the wave-vector length. Consequently, GVD-cancellation via angular dispersion has not been demonstrated to date in the anomalous dispersion regime. We synthesize here structured femtosecond pulsed beams known as ‘space-time’ wave packets designed to realize dispersion-cancellation symmetrically in either the normal- or anomalous-GVD regimes by virtue of non-differentiable angular dispersion inculcated into the pulsed field. Furthermore, we also verify GVD-inversion: reversing the GVD sign experienced by the field with respect to that dictated by the chromatic dispersion of the medium itself.

## I. INTRODUCTION

Chromatic dispersion resulting from the wavelength-dependence of the refractive index is an inescapable feature of optical materials, which leads to pulse broadening and distortion [1, 2]. One may combat its impact via dispersion *compensation* or dispersion *cancellation*. In the former, dispersive broadening and the associated chirp are compensated after (or pre-compensated before) passage through the medium, which is key to the success of chirped pulsed amplification (CPA) [3], for example. Normal group-velocity dispersion (GVD) can be compensated by a pair of gratings or prisms [4], anomalous GVD by a Martinez stretcher [5], and almost arbitrary dispersion by a 4f pulse shaper or other techniques [6–11]. In all these cases, it is the group delay dispersion (GDD) that is being neutralized. More challenging, however, is to neutralize dispersion *during* passage through a dispersive medium, so that the pulse travels invariantly, which we refer to as *dispersion cancellation*. Such a capability is crucial, for instance, in enabling efficient nonlinear interactions in long crystals. Angular dispersion [12], whereby each frequency in the pulse is directed at a prescribed angle, has been successfully utilized for this purpose [13]. The resulting field structure after inculcating angular dispersion is typically known as a tilted pulse front (TPF) [14]. To date, however, angular dispersion has been used for dispersion cancellation in only the *normal*-GVD regime. There have been no reports of dispersion-cancellation in the anomalous-GVD regime, and well-established theoretical considerations suggest the impossibility of such a goal [15]. Indeed, there is strong *a priori* conceptual support for such a claim. Because normal GVD *increases* the wave-vector length in the dispersive medium by a frequency-dependent amount, Changing the wave-vector angle for each frequency can reduce its axial component to the pre-GVD value. Anomalous GVD, on the other hand, *reduces* the wave-vector length, and no angular tilt can com-

pensate for such a reduction. Consequently, cancelling anomalous GVD has *not* been reported to date.

Nevertheless, pulsed beams or wave packets that are propagation invariant (diffraction-free and dispersion-free) in dispersive media by virtue of their spatio-temporal field structure have been known to exist theoretically [16–21] in presence of normal *and* [22] anomalous [23] GVD. These sought-after dispersion-free structured fields have *not* been observed to date in linear dispersive media, although there is evidence for their presence in nonlinear interactions [24–27]. Such spatiotemporally structured fields have been recently studied systematically in free space and non-dispersive dielectrics under the rubric of ‘space-time’ (ST) wave packets [28–34]. These propagation-invariant wave packets feature a unique set of characteristics including tunable group velocities in absence of chromatic dispersion [35–38], self-healing [39], anomalous refraction [40–44], and novel ST Talbot effects [45]. The central characteristics of ST wave packets in free space are now well-understood [34, 46], and potential applications are being evaluated in optical communications [47, 48] and device physics [49–55].

In contrast to TPFs, the angular dispersion undergirding ST wave packets is ‘non-differentiable’: the derivative of the propagation angle is *not* defined at one wavelength [56–58]. Such angular dispersion can be produced by a recently developed pulsed-beam shaper that serves as a universal angular-dispersion synthesizer in one dimension [59]. We have recently shown that non-differentiable angular dispersion is the crucial ingredient for tuning the group velocity of a ST wave packet and introducing an arbitrary dispersion profile in free space [57, 60]. This suggests the prospect for dispersion-cancellation in presence of either normal- or anomalous-GVD.

Here, we verify the propagation invariance of ST wave packets symmetrically in *both* the normal- *and* anomalous-GVD regimes, the latter for the first time to the best of our knowledge. We identify the spatio-temporal spectral structures needed for achieving GVD-cancellation. The crucial step is to first change the ST

wave-packet group velocity via non-differentiable angular dispersion, which opens up a space for subsequent decrease or increase in the axial wave vector relative to the dispersion-free configuration. We sculpt the spatio-temporal spectrum of  $\approx 200$ -fs ( $\approx 16$ -nm-bandwidth) pulses to produce ST wave packets that are propagation invariant at a wavelength of  $\approx 1 \mu\text{m}$  in ZnSe as a representative normal-GVD medium, and chirped Bragg mirrors that produce anomalous GVD. Uniquely, the GVD in the medium is cancelled while maintaining independent control over the group velocity of the ST wave packet (in both the subluminal and superluminal regimes). Furthermore, not only is propagation invariance achieved in dispersive media, but dispersion inversion is also verified: the sign of GVD experienced by the wave packet in the medium is *reversed*. We thus produce wave packets that undergo normal GVD in an anomalously dispersive medium, and vice versa. We expect these results to be particularly useful in tailoring multi-wavelength nonlinear optical interactions in long crystals.

## II. THE CHALLENGE OF CANCELING ANOMALOUS GVD VIA ANGULAR DISPERSION

Angular dispersion, whereby each frequency  $\omega$  in a pulsed field travels at a different angle  $\varphi(\omega)$  [12], produces anomalous GVD in free space [4, 15, 61], which can help cancel normal GVD [13, 16]. In fact, it is commonly understood that angular dispersion *cannot* produce normal GVD in free space [15], and thus does not provide the possibility of cancelling anomalous GVD. The illustration in Fig. 1 elucidates the origin of this asymmetry between realizing normal and anomalous GVD via conventional angular dispersion.

Consider a plane-wave pulse traveling in a dispersive medium of refractive index  $n(\omega)$ , and expand the wave number  $k(\omega) = n(\omega)\omega/c$  around a frequency  $\omega_o$ ,  $k(\omega_o + \Omega) \approx n_m k_o + \frac{\Omega}{\tilde{v}_m} + \frac{1}{2}k_{2m}\Omega^2$ ; here  $\Omega = \omega - \omega_o$ ,  $k_o = \omega_o/c$ ,  $c$  is the speed of light in vacuum,  $n_m = n(\omega_o)$ ,  $\tilde{v}_m = 1/\frac{dk}{d\omega}|_{\omega_o} = \frac{c}{\tilde{n}_m}$  is the group velocity and  $\tilde{n}_m$  the group index, and  $k_{2m} = \frac{d^2k}{d\omega^2}|_{\omega_o}$  is the GVD coefficient [1]. Throughout, we use the subscript ‘m’ to denote quantities in the dispersive medium, and the subscript ‘a’ for the corresponding quantities in free space. It is clear that normal GVD  $k_{2m} > 0$  *increases* the wave-vector length by a frequency-dependent amount  $\frac{1}{2}k_{2m}\Omega^2$  [Fig. 1(a)], which can be counterbalanced by tilting the wave vector by an angle  $\varphi_m(\omega)$  to *reduce* the axial component of the wave vector in the medium to the pre-GVD value  $k_z(\omega) = k(\omega) \cos\{\varphi_m(\omega)\} \approx n_m k_o + \frac{\Omega}{\tilde{v}_m}$  [Fig. 1(b)]. To realize this condition in the small-angle limit starting with a plane-wave pulse in free space [Fig. 1(c)], we tilt the wave vector associated with  $\omega$  by an angle  $\varphi_a(\Omega) \approx \frac{\Omega}{\omega_o} \tan \delta_a^{(1)}$  [Fig. 1(d,e)], where  $\delta_a^{(1)}$  is the tilt angle of the pulse front (the plane of constant amplitude)

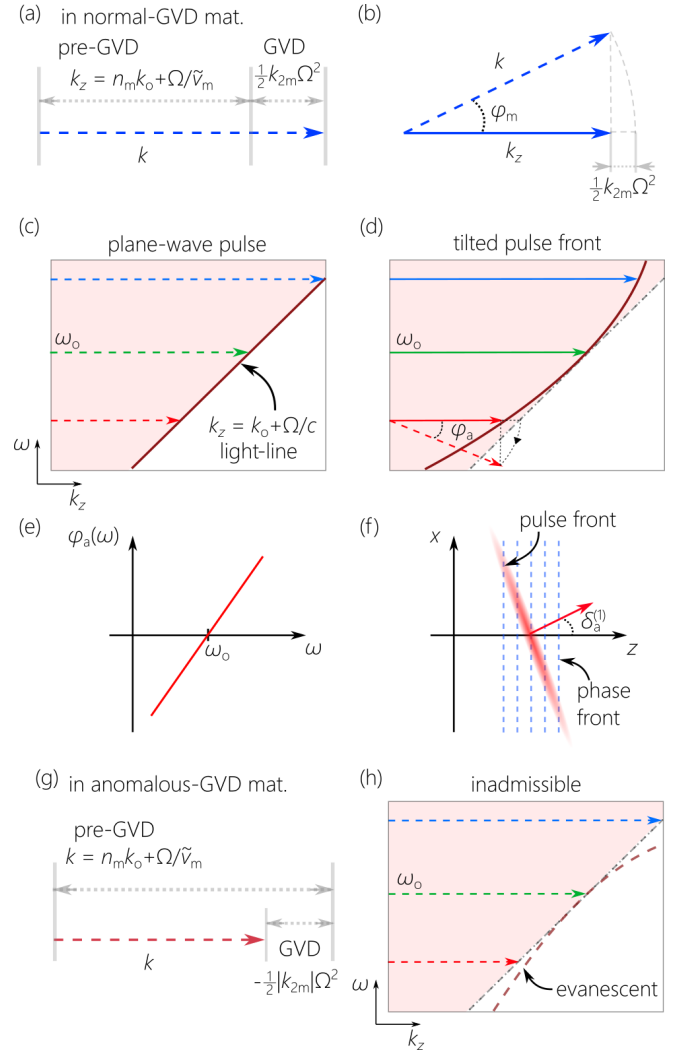


FIG. 1. (a) Normal GVD *increases* the wave-vector length, (b) but angular dispersion reduces the axial wave-vector component  $k_z$  to the pre-GVD value. (c) In free space,  $k(\omega) = \frac{\omega}{c} = k_o + \frac{\Omega}{c}$ , and (d) after rotating  $k(\omega)$  by an angle  $\varphi_a(\omega)$ , the field experiences anomalous GVD in free space. (e) The requisite angle introduced into the plane-wave pulse in free space is  $\varphi_a(\omega) = \varphi_a(\omega_o + \Omega) \propto \Omega$ . (f) The angular dispersion in (e) produces a field in the form of a tilted pulse front (TPF). (g) In the *anomalous*-GVD regime, the angular-dispersion approach fails because the wave-vector length is *reduced*, and a tilt *cannot* increase  $k_z$  to its pre-GVD value. (h) Introducing normal GVD into a plane-wave pulse in free space via conventional angular dispersion renders the field evanescent.

with respect to the phase front (the plane of constant phase) [Fig. 1(f)]. Such a field structure is known as a TPF [14], which in general experiences *anomalous* GVD in free space  $k_{2a} = -\frac{1}{c\omega_o} \tan^2 \delta_o^{(1)}$  [16]. Once coupled to a medium in its normal-GVD regime, the TPF propagates dispersion-free if  $k_{2a} = -n_m k_{2m}$  (Appendix).

The challenge of cancelling *anomalous* GVD  $k_{2m} < 0$  is now clear. Anomalous GVD *reduces*  $k(\omega)$  in the medium by  $-\frac{1}{2}k_{2m}\Omega^2$  [Fig. 1(g)], and no angular tilt can *increase*

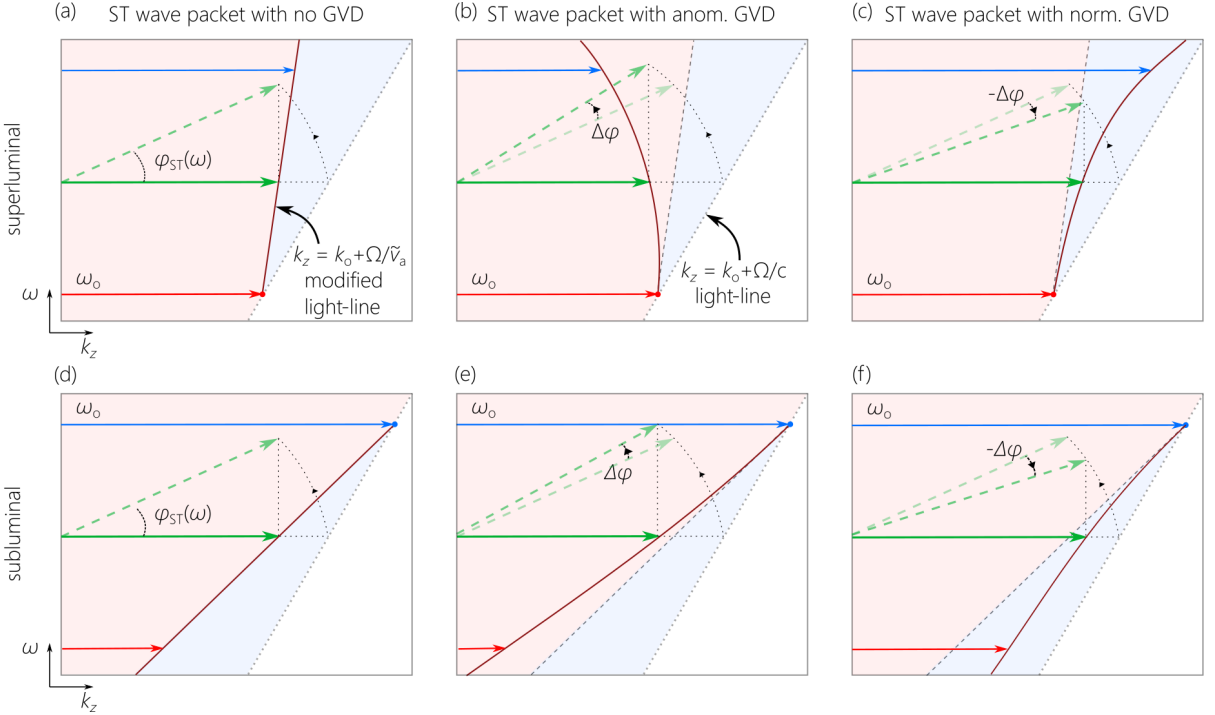


FIG. 2. The impact of *non-differentiable* angular dispersion on the group velocity and GVD in free space. (a) By introducing a tilt angle  $\varphi_{\text{ST}}(\omega_0 + \Omega) \approx \eta\sqrt{\Omega/\omega_0}$  into a plane-wave pulse, the group velocity becomes  $\tilde{v} = c/\tilde{n}_a$ , and  $k_z$  is determined by a modified light-line  $k_z = k_0 + \Omega/\tilde{v}_a$  rather than the free-space light-line  $k_z = \frac{\omega}{c} = k_0 + \Omega/c$ . (b) By further increasing the tilt angle to  $\varphi_{\text{ST}} + \Delta\varphi$ ,  $k_z$  is reduced and determined by a quadratic curve consistent with anomalous GVD in free space. (c) By reducing the tilt angle to  $\varphi_{\text{ST}} - \Delta\varphi$ ,  $k_z$  is increased and determined by a quadratic curve consistent with normal GVD. Such scenarios can be achieved only via non-differentiable angular dispersion. Panels (a-c) correspond to superluminal and (d-f) to subluminal ST wave packets.

$k_z$  to the pre-GVD value. As shown in Fig. 1(h), the dispersion curve for normal GVD in free space lies *below* the light-line, corresponding to an evanescent field. Although this appears to be an insurmountable obstacle, we show here that it is resolved by ST wave packets endowed with *non-differentiable* angular dispersion.

### III. THEORY OF PROPAGATION-INVARIANT SPACE-TIME WAVE PACKETS IN DISPERSIVE MEDIA

#### A. Symmetrized anomalous and normal GVD in free space via angular dispersion

The key to introducing anomalous *or* normal GVD symmetrically into a pulsed field is to first change the group velocity along the propagation axis, which is given by:  $\tilde{v}_a = c/\{\cos\varphi_0 - \omega_0\varphi_0^{(1)}\sin\varphi_0\}$ ; where  $\varphi_0 = \varphi_a(\omega_0)$  and  $\varphi_0^{(1)} = \frac{d\varphi_a}{d\omega}\big|_{\omega_0}$  [16]. For on-axis propagation  $\varphi_0 \rightarrow 0$ ,  $\tilde{v}_a \rightarrow c$  for any finite value of  $\varphi_0^{(1)}$ . However, setting  $\varphi_a(\omega) = \varphi_{\text{ST}}(\omega_0 + \Omega) \approx \eta\sqrt{\Omega/\omega_0}$ , which is *not* differentiable at  $\omega = \omega_0$ , yields a propagation-invariant ST wave packet with a group velocity  $\tilde{v}_a = \frac{c}{\tilde{n}_a}$  and group index

$\tilde{n}_a = 1 - \frac{1}{2}\eta^2$ , where  $\eta$  is a frequency-independent constant [57, 58]. For a superluminal ST wave packet  $\tilde{v}_a > c$ ,  $\omega_0$  is the minimum frequency in the spectrum [Fig. 2(a)]; and for the subluminal counterpart  $\tilde{v}_a < c$ ,  $\omega_0$  is the maximum [Fig. 2(d)]. The axial wave numbers are now limited by the modified light-line  $k_z(\omega) = \frac{\omega}{c} \cos\varphi_{\text{ST}} = k_0 + \frac{\Omega}{\tilde{v}_a}$  rather than the free-space light-line  $k_z = k_0 + \frac{\Omega}{c}$  [Fig. 2(a,d)]. Because  $k_z$  is linear in  $\Omega$ , the ST wave packet is dispersion-free.

It can now be appreciated how anomalous *or* normal GVD are induced in free space. Anomalous GVD requires reducing  $k_z$  by further increasing the angular tilt,  $\varphi_{\text{anom}}(\omega) = \varphi_{\text{ST}}(\omega) + \Delta\varphi(\omega)$ , with respect to the GVD-free configuration [Fig. 2(b,e)]. This regime is also accessible via conventional TPFs. In contrast, normal GVD requires increasing  $k_z$  with respect to the GVD-free configuration by reducing the angular tilt  $\varphi_{\text{norm}}(\omega) = \varphi_{\text{ST}}(\omega) - \Delta\varphi(\omega)$  [Fig. 2(c,f)]. Because of the space that opened up above the free-space light-line  $k_z = k_0 + \Omega/c$  but below the modified light-line  $k_z = k_0 + \Omega/\tilde{v}_a$ , we can increase  $k_z$  without the field becoming evanescent. This regime is inaccessible to TPFs [Fig. 1(h)] or other structured pulsed fields, and requires non-differentiable angular dispersion for its realization.

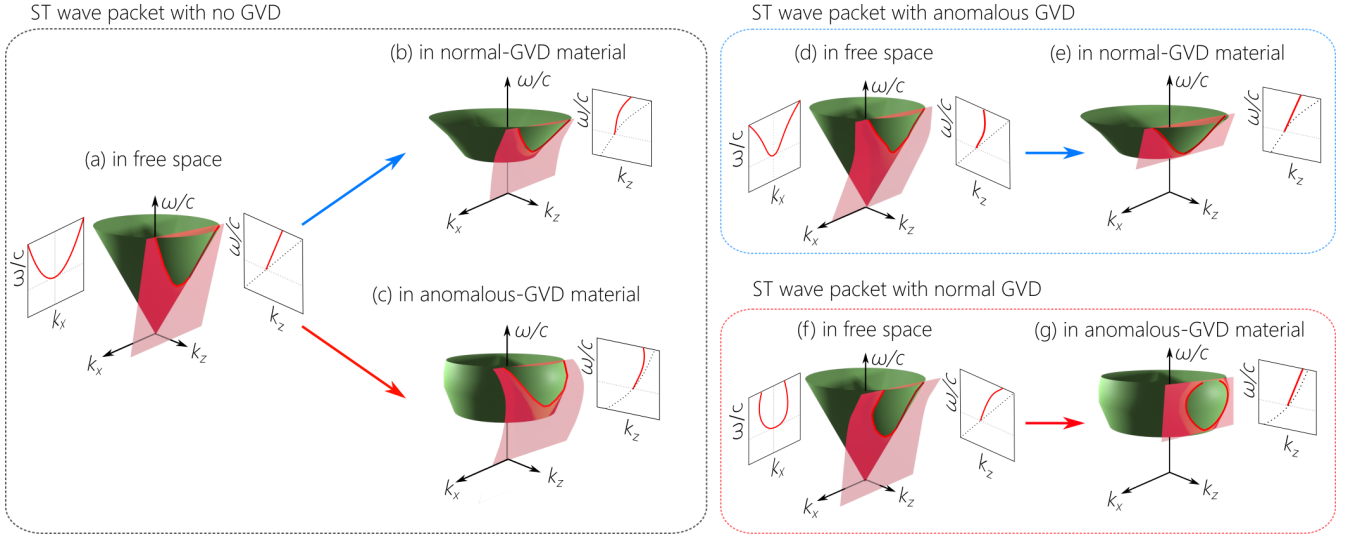


FIG. 3. (a) The spectral support domain of a propagation-invariant ST wave packet in free space on the surface of the light-cone  $k_x^2 + k_z^2 = (\frac{\omega}{c})^2$ , and its projections onto the  $(k_x, \frac{\omega}{c})$  and  $(k_z, \frac{\omega}{c})$  planes. The  $(k_z, \frac{\omega}{c})$ -projection is a straight line, indicating absence of dispersion [Fig. 2(a)]. (b) The ST wave packet from (a) after coupling to a normal-GVD or (c) an anomalous-GVD medium. The  $(k_z, \frac{\omega}{c})$ -projections are now curved, indicating that the wave packet in the medium is dispersive. The  $(k_x, \frac{\omega}{c})$ -projections are all the same in (a-c). (d) The spectral support domain for a ST wave packet endowed with *anomalous* GVD in free space [Fig. 2(b)]. The  $(k_z, \frac{\omega}{c})$ -projection is no longer a straight line as in (a). (e) The ST wave packet from (d) after coupling to a medium with *normal* GVD. The  $(k_z, \frac{\omega}{c})$ -projection has been ‘straightened out’, thus indicating dispersion-cancellation. (f) The spectral support domain for a ST wave packet endowed with *normal* GVD in free space. (g) The ST wave packet from (f) after coupling to a medium with *anomalous* GVD. Once again, The  $(k_z, \frac{\omega}{c})$ -projection has been ‘straightened out’. In each case, the spectral projection onto the  $(k_x, \frac{\omega}{c})$ -plane is invariant across the interface between free space and the dispersive medium.

## B. Coupling from free space to a dispersive medium

To analyze quantitatively the scenario illustrated in Fig. 2, the representation of the spectral support domain of pulsed fields on the surface of the light-cone is a useful guide [34, 62]. In free space, the light-cone is  $k_x^2 + k_z^2 = (\frac{\omega}{c})^2$ , where  $k_x$  is the transverse wave number or spatial frequency (we hold the field uniform along  $y$  for simplicity). The spectral support domain for a propagation-invariant ST wave packet traveling at a group velocity  $\tilde{v}_a$  is the intersection of the light-cone with a plane  $k_z = k_o + \Omega/\tilde{v}_a$  that is parallel to the  $k_x$ -axis and makes an angle  $\theta_a$  (the spectral tilt angle) with the  $k_z$ -axis [36, 63, 64], where  $\tilde{v}_a = c \tan \theta_a$  [Fig. 3(a)]. The spectral projection onto the  $(k_z, \frac{\omega}{c})$ -plane is a straight line, and onto the  $(k_x, \frac{\omega}{c})$ -plane is a conic section that can be approximated by a parabola in the vicinity of  $k_x = 0$  in the paraxial regime [37, 64].

In presence of GVD due to chromatic dispersion, the dispersion relationship  $k_x^2 + k_z^2 = (n\frac{\omega}{c})^2$  corresponds to a modified light-cone [Fig. 3(b,c)]. At normal incidence on a planar interface,  $k_x$  and  $\Omega$  are invariant, so the  $(k_x, \frac{\omega}{c})$ -projection is the same in free space and the dispersive

medium:

$$k_x^2 = \underbrace{\frac{\omega^2}{c^2} - \left(k_o + \frac{\Omega}{\tilde{v}_a}\right)^2}_{\text{in free space}} = \underbrace{\left(n_m k_o + \frac{\Omega}{\tilde{v}_m} + \frac{1}{2} k'_{2m} \Omega^2\right)^2}_{\text{in the medium}} - k_z^2. \quad (1)$$

However, the  $(k_z, \frac{\omega}{c})$ -projection changes because the light-cone structure has been modified. The ST wave packet that was propagation-invariant in free space now experiences GVD in the dispersive medium. We expand the axial wave number in the medium as  $k_z \approx n_m k_o + \frac{\Omega}{\tilde{v}} + \frac{1}{2} k'_{2m} \Omega^2$ , where  $\tilde{v} = \frac{c}{\tilde{n}}$  is the group velocity of the ST wave packet in the medium (which need not be equal to  $\tilde{v}_m$ ), and  $k'_{2m}$  is the effective GVD coefficient (which can differ from the GVD coefficient  $k_{2m}$  in the medium).

By equating the *first-order*  $\Omega$  terms in Eq. 1, we obtain:

$$1 - \tilde{n}_a = n_m (\tilde{n}_m - \tilde{n}), \quad (2)$$

which can be recognized as the law of refraction for a ST wave packet in a dispersive medium derived in [65, 66] that governs the change in group velocity from  $\tilde{v}_a = \frac{c}{\tilde{n}_a}$  in free space to  $\tilde{v} = \frac{c}{\tilde{n}}$  in the medium. Indeed, the quantity  $n_m (\tilde{n}_m - \tilde{n})$  is a refractive invariant for ST wave packets at normal incidence on planar interfaces between dispersive media, which we have called the ‘spectral curvature’ because it is related to the curvature of the parabolic

$(k_x, \frac{\omega}{c})$ -projection in the vicinity of  $k_x=0$ . This relationship indicates that a subluminal ST wave packet in free space  $\tilde{v}_a < c$  remains subluminal in the medium  $\tilde{v} < \tilde{v}_m$ , and similarly for superluminal wave packets.

Equating the *second-order*  $\Omega^2$  terms in Eq. 1 yields a relationship between the GVD coefficient of the medium  $k_{2m}$  and the effective GVD coefficient experienced by the wave packet  $k'_{2m}$ :

$$k'_{2m} = k_{2m} + \frac{1}{n_m} \frac{\Delta}{c\omega_o}. \quad (3)$$

From this we conclude that the ST wave packet experiences the normal or anomalous GVD intrinsic to the medium itself [Fig. 3(b,c)] except for an offset term:

$$\Delta = (\tilde{n}_m^2 - \tilde{n}^2) - (1 - \tilde{n}_a^2). \quad (4)$$

In most cases where the deviation from the luminal limit is small ( $\tilde{n}_a \rightarrow 1$  and  $\tilde{n} \rightarrow \tilde{n}_m$ ),  $\Delta$  can be ignored, and we have  $k'_{2m} \approx k_{2m}$ .

### C. Achieving dispersion-free propagation in presence of GVD

Dispersion-free propagation in the dispersive medium is achieved by modifying the structure of the ST wave packet in free space to introduce GVD of opposite sign to that of the medium: cancelling normal GVD necessitates endowing the ST wave packet in free space with anomalous GVD [Fig. 3(d,e)], and vice versa [Fig. 3(f,g)]. In free space, the  $(k_z, \frac{\omega}{c})$ -projection is no longer a straight line, but rather takes the form  $k_z = k_o + \frac{\Omega}{\tilde{v}_a} + \frac{1}{2}k_{2a}\Omega^2$ , where  $k_{2a}$  is the GVD coefficient introduced into the ST wave packet. The spectral support domain on the free-space light-cone is its intersection with a planar *curved* surface that is parallel to the  $k_x$ -axis:

$$k_x^2 + \left( k_o + \frac{\Omega}{\tilde{v}_a} + \frac{1}{2}k_{2a}\Omega^2 \right)^2 = \left( k_o + \frac{\Omega}{c} \right)^2. \quad (5)$$

The change in the light-cone structure in the medium in conjunction with the invariance of the  $(k_x, \frac{\omega}{c})$ -projection can yield a  $(k_z, \frac{\omega}{c})$ -projection in the medium that is a *straight line*. In other words, the curved  $(k_z, \frac{\omega}{c})$ -projection in free space has been ‘straightened out’ in the medium such that  $k_z = n_mk_o + \frac{\Omega}{\tilde{v}}$ , thus signifying dispersion-free propagation in the medium:

$$k_x^2 + \left( n_mk_o + \frac{\Omega}{\tilde{v}} \right)^2 = \left( n_mk_o + \frac{\Omega}{\tilde{v}_m} + \frac{1}{2}k_{2m}\Omega^2 \right)^2. \quad (6)$$

Equating the  $\Omega$ -terms in Eq. 5 and Eq. 6 yields  $1 - \tilde{n}_a = n_m(\tilde{n}_m - \tilde{n})$  as in Eq. 2), whereas equating the  $\Omega^2$ -terms yields:

$$k_{2a} = -n_mk_{2m} - \frac{\Delta}{c\omega_o}. \quad (7)$$

That is, dispersion cancellation requires that the dispersion coefficient introduced in free space  $k_{2a}$  must have the opposite sign to that of the medium  $k_{2m}$ , and to be weighted by the refractive index  $n_m$ . This result is similar to that for a TPF (Appendix) except that the GVD to be cancelled can be *either* normal *or* anomalous (in addition to the minor offset term  $\Delta$ ).

## IV. EXPERIMENT

### A. Spatio-temporal spectral synthesis

To synthesize dispersive ST wave packets in free space, we make use of the universal angular-dispersion synthesizer described in [59] and depicted in Fig. 4. We start with plane-wave femtosecond pulses of width  $\approx 100$  fs and bandwidth  $\approx 25$  nm at a central wavelength of  $\lambda_o \approx 1064$  nm (Spark Lasers; Alcor). The pulses are spectrally resolved via a diffraction grating (1200 lines/mm) followed by a collimating cylindrical lens of focal length  $f=500$  mm. At the focal plane of the lens we place a reflective, phase-only spatial light modulator (SLM; Meadowlark, E19X12) that imparts a 2D phase distribution to the impinging spectrally resolved wave front. Each wavelength occupies a column on the SLM, along which we impose the phase  $\Phi(x, \lambda) = \pm \frac{2\pi}{\lambda} \sin\{\phi(\lambda)\}x$ , where  $\phi(\lambda)$  is the deflection angle for  $\lambda$  with respect to the  $z$ -axis. An example of the phase pattern  $\Phi(x, \lambda)$  is depicted in Fig. 4, inset. The upper half of each SLM column deflects the wavelength  $\lambda$  at an angle  $\phi(\lambda)$ , while the lower half deflects it at  $-\phi(\lambda)$ . This yields a symmetric spatio-temporal angular spectrum  $\varphi(\lambda)$  [Fig. 4, inset], and produces a X-shaped wave-packet profile, whereas that for TPFs [Fig. 1(f)] comprises one branch of the X-shaped profile. The wave front retro-reflected from the SLM returns to the grating where the ST wave packet is formed, and the dispersive sample is placed in its path.

### B. Dispersive samples

The normal-GVD medium is ZnSe (Thorlabs; WG71050) formed of multiple 1-inch-diameter discs of thickness 5 mm each, stacked to a maximum thickness of 30 mm. Using the Sellmeier equation for ZnSe,  $n^2(\lambda) = 4 + \frac{1.9\lambda^2}{\lambda^2 - 0.113}$  ( $\lambda$  in units of  $\mu\text{m}$ ) [67], we obtain at  $\lambda_o = 1064$  nm an index  $n_m \approx 2.49$ , group index  $\tilde{n}_m \approx 2.57$ , and GVD parameter  $k_{2m} \approx +607.45$  fs<sup>2</sup>/mm. It is useful to exploit the dimensionless GVD parameter  $c\omega_o k_{2m} \approx 0.32$ .

The anomalous-GVD sample comprises a pair of chirped Bragg mirrors (Edmund Optics, 12-335) that generate -1000 fs<sup>2</sup> group delay dispersion (GDD) per reflection. By changing the distance separating the two mirrors, we can increase the number of reflections for a given propagation distance before the wave packet

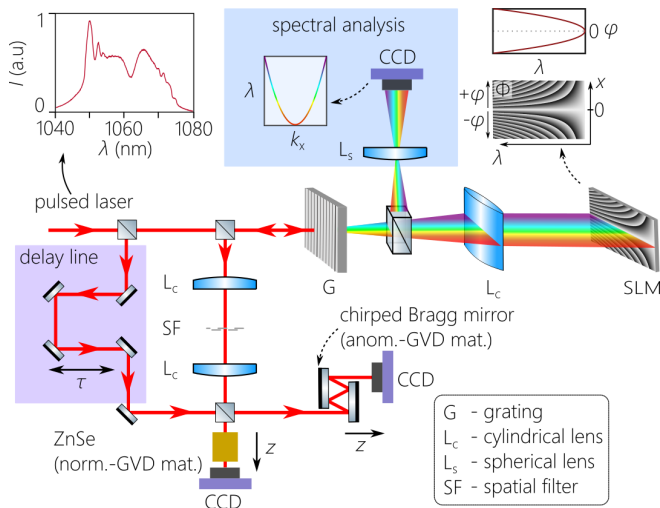


FIG. 4. Schematic of the setup for synthesizing and characterizing dispersive ST wave packets. The inset in the upper left corner is the spectrum of the pulsed laser used. The insets in the upper right corner depict the two-dimensional phase pattern  $\Phi$  imparted by the SLM to the spectrally resolved wave front, and the resulting angular dispersion  $\varphi(\lambda)$  inculcated into the incident field.

emerges, thus controllably increasing the GDD from  $-2000$  to  $-15000$   $\text{fs}^2$ . The GVD is then taken to be the GDD divided by the total length propagated at a fixed incident angle of  $7^\circ$ , resulting in an effective GVD coefficient of  $k_{2m} \approx -500$   $\text{fs}^2/\text{mm}$  and a medium length extending up to  $30$  mm. The dimensionless GVD parameter here is  $c\omega_0 k_{2m} \approx -0.25$ , and  $n_m \approx \tilde{n}_m \approx 1$  because the ST wave packet travels predominantly in free space.

## V. SPECTRAL MEASUREMENTS

The spatio-temporal spectrum projected onto the  $(k_x, \lambda)$ -plane is obtained after implementing a spatial Fourier transform on the spectrally resolved wave front reflecting back from the SLM [Fig. 4]. The intensity distribution is then recorded by a CCD camera. The result is a parabola centered at  $k_x = 0$  of spatial bandwidth  $\Delta k_x \approx 0.23$   $\text{rad}/\mu\text{m}$  (corresponding to a spatial width of  $\Delta x \approx 20$   $\mu\text{m}$  at the pulse center) and a temporal bandwidth of  $\Delta \lambda \approx 16$  nm (corresponding to a temporal linewidth of  $\Delta T \approx 200$  fs at the beam center). We plot in Fig. 5 the measured spectra for two classes of ST wave packets: subluminal in Fig. 5(a,c,e) with  $\theta_a = 44^\circ$  and  $\tilde{v}_a \approx 0.96c$ , and superluminal in Fig. 5(b,d,f) with  $\theta_a = 46^\circ$  and  $\tilde{v}_a \approx 1.04c$ . In each category we produce three distinct wave packets in free space: (1) a GVD-free wave packet that is propagation invariant [Fig. 5(a,b)]; (2) a dispersive ST wave packet endowed with *anomalous* GVD  $k_{2a} < 0$  [Fig. 5(c,d)]; and (3) a dispersive ST wave packet endowed with *normal* GVD  $k_{2a} > 0$  in free space [Fig. 5(e,f)]. In all cases, each spatial frequency  $k_x$  is

associated with a single wavelength  $\lambda$ . After introducing anomalous GVD  $k_{2a} < 0$ ,  $|k_x|$  increases with respect to its GVD-free counterpart, corresponding to the required increase in propagation angle [Fig. 2(b,e)]. Alternatively,  $|k_x|$  decreases with respect to the GVD-free wave packet after incorporating normal GVD  $k_{2a} > 0$  [Fig. 5(e,f)] corresponding to the required decrease in propagation angle [Fig. 2(c,f)].

From these spectra in the  $(k_x, \lambda)$ -plane, we extract the spectral projection onto the  $(k_z, \lambda)$ -plane for the field in free space, making use of the relationship  $k_z^2 = (\frac{\omega}{c})^2 - k_x^2$ . This spectral projection for the GVD-free wave packets is a straight line [Fig. 5(a,b)]. These wave packets propagate invariantly in free space. However, the  $(k_z, \lambda)$ -projections curve away from that straight line in presence of GVD [Fig. 5(c-f)]. The dashed lines in the  $(k_z, \lambda)$ -plane [Fig. 5(c-f)] are the modified light-lines  $k_z = k_0 + \Omega/\tilde{v}_a$ . Introducing anomalous GVD reduces  $k_z$ , whereas incorporating normal GVD increases  $k_z$  at each wavelength, which is consistent with our goal as illustrated in Fig. 2. Therefore, the measurements confirm that the targeted spatio-temporal spectra have indeed been produced in free space. We now proceed to verify that the expected propagation dynamics is produced in free space and in the dispersive media.

## VI. DISPERSIVE SPACE-TIME WAVE PACKETS IN FREE SPACE

We reconstruct the spatio-temporal envelope of the wave-packet intensity profile  $I(x, z; \tau)$  at a given axial plane  $z$  via linear interferometry making use of the initial laser pulses as a reference [36]; see Fig. 4. When the ST wave packet and the reference pulse overlap in space and time, spatially resolved fringes are recorded by a CCD camera whose visibility is used to reconstruct the wave packet profile as an optical delay  $\tau$  is swept in the path of the reference pulse. Furthermore, the profiles of the ST wave packet at different axial planes  $z$  are reconstructed by displacing the CCD camera to the target plane  $z$  and compensating for the relative group delay between the ST wave packet (travelling at  $\tilde{v}_a = c \tan \theta_a$ ) and the reference pulse (travelling at  $c$ ).

We start off with a subluminal ( $\theta_a = 44^\circ$ ) propagation-invariant ST wave packet in free space, and plot in Fig. 6(a) the measured profile  $I(x, z; \tau)$  at three axial planes in free space ( $z = 0, 15, \text{ and } 30$  mm) reconstructed in a frame traveling at  $\tilde{v}_a$ . The X-shaped ST wave packet travels invariantly without distortion. The on-axis pulsewidth is constant in free space at  $\Delta T \approx 200$  fs. However, once this wave packet is coupled to a dispersive medium, pulse broadening is observed; see Fig. 6(b) for the normal-GVD medium and Fig. 6(c) for its anomalous-GVD counterpart. The pulsewidth increases monotonically from  $\Delta T \approx 200$  fs to  $\Delta T \approx 600$  fs after  $30$  mm in either medium [Fig. 6(d,e)].

Crucially, accompanying pulse broadening is an asym-

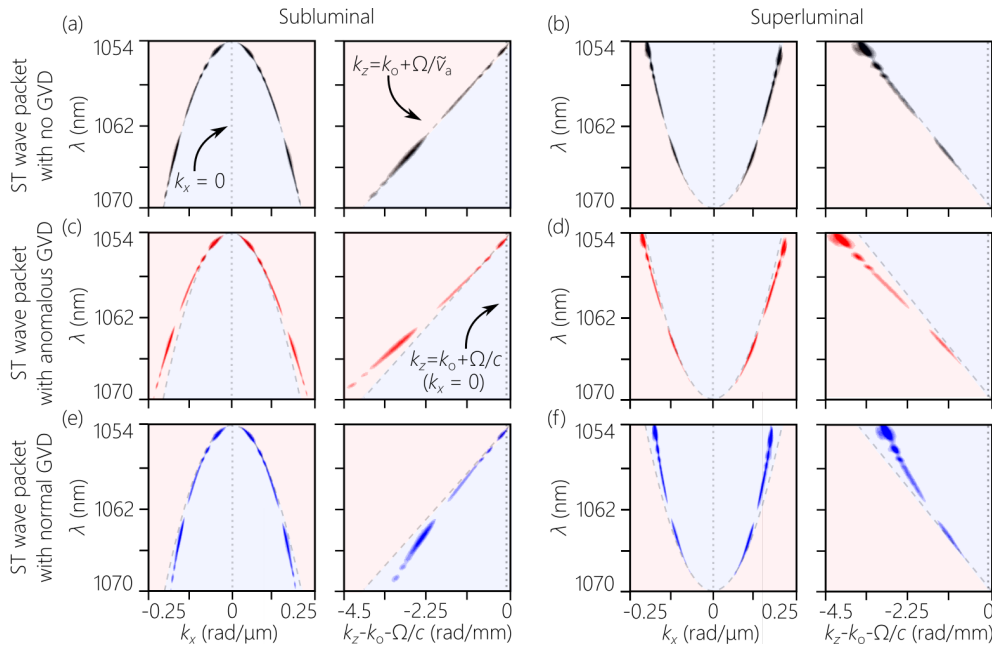


FIG. 5. Measured spectral projections onto the  $(k_x, \lambda)$  and  $(k_z, \lambda)$  planes, (a,c,e) for subluminal wave packets with  $\theta_a = 44^\circ$  and  $\tilde{v}_a = 0.96c$ , and (b,d,f) for superluminal wave packets with  $\theta_a = 46^\circ$  and  $\tilde{v}_a = 1.04c$ . (a,b) Dispersion-free ST wave packets in free space; (c,d) ST wave packets endowed with anomalous GVD in free space,  $c\omega_o k_{2a} = -0.8$ ; and (e,f) ST wave packets endowed with anomalous GVD in free space,  $c\omega_o k_{2a} = 0.8$ . The dotted curves in the  $(k_x, \lambda)$ -plane are the theoretical spectra of the GVD-free wave-packets in (a) and (b), and are a guide for the eye in the case of their dispersive counterparts. The dashed lines in the  $(k_z, \lambda)$ -plane are the modified light-lines  $k_z = k_o + \frac{\Omega}{\tilde{v}_a}$ . The free-space light-line is the vertical axis at  $k_z - k_o - \frac{\Omega}{c} = 0$ .

metry between the structure of the wave packets in the normal- and anomalous-GVD media in regards to the direction of pulse broadening. In a normal-GVD medium, the pulse broadens towards later delays with respect to  $\tau = 0$ , whereas it broadens towards advanced delays. The distinct field structures that emerge in these two cases allow us to unambiguously delineate the wave packet at the output of the anomalous- and normal-GVD media. In Fig. 6(d) we plot the on-axis pulse profiles  $I(0, z; \tau)$  at  $z = 0, 15$  mm, and 30 mm for the wave packets in Fig. 6(a-c) to highlight this asymmetry, which provides a clear signature of the type of GVD experienced by the wave packet. Note, however, that the rate of increase in pulsewidth  $\Delta T$  with distance [Fig. 6(e)] does *not* depend on the sign of the GVD [1].

## VII. PROPAGATION INVARIANCE IN DISPERSIVE MEDIA

### A. Normal-GVD cancellation

GVD-free propagation in ZnSe in the normal-GVD regime requires introducing anomalous GVD into the ST wave packet in free space. We set  $k_{2a} \approx -1500$  fs<sup>2</sup>/mm ( $c\omega_o k_{2m} \approx -0.8$ ) for a subluminal ST wave packet and monitor its propagation in free space, whereupon it exhibits dispersive temporal broadening [Fig. 7(a)]. Moreover, the temporal asymmetry exhibited by the wave

packet confirms that it experiences anomalous GVD in free space; compare Fig. 7(a) to Fig. 6(c). However, once the wave packet is coupled to ZnSe, this behavior is halted, and the wave packet travels GVD-free with a propagation-invariant spatio-temporal profile independently of the distance up to a 30-mm-thick ZnSe sample [Fig. 7(b)]. The on-axis pulse broadening in free space depicted in Fig. 7(c,d) is in quantitative agreement with the expectation based on the GVD coefficient introduced, whereas the pulsewidth is constant after GVD-cancellation.

### B. Anomalous-GVD cancellation

Propagation invariance in the anomalous-GVD sample requires introducing normal GVD into the ST wave packet in free space. Setting  $k_{2a} \approx 500$  fs<sup>2</sup>/mm ( $c\omega_o k_{2m} \approx 0.25$ ) and monitoring the propagation of the dispersive ST wave packet in free space reveals dispersive temporal broadening [Fig. 7(e)]. The temporal asymmetry in the wave packet spreading is consistent with normal GVD [compare Fig. 7(e) to Fig. 6(b)]. However, after traversing the chirped mirrors, the wave packet travels GVD-free with a propagation-invariant spatio-temporal profile independently of the sample thickness [Fig. 7(f)]. Once again, the broadening in the on-axis pulsewidth  $\Delta T$  is in quantitative agreement with the expectation based on the GVD coefficient introduced,

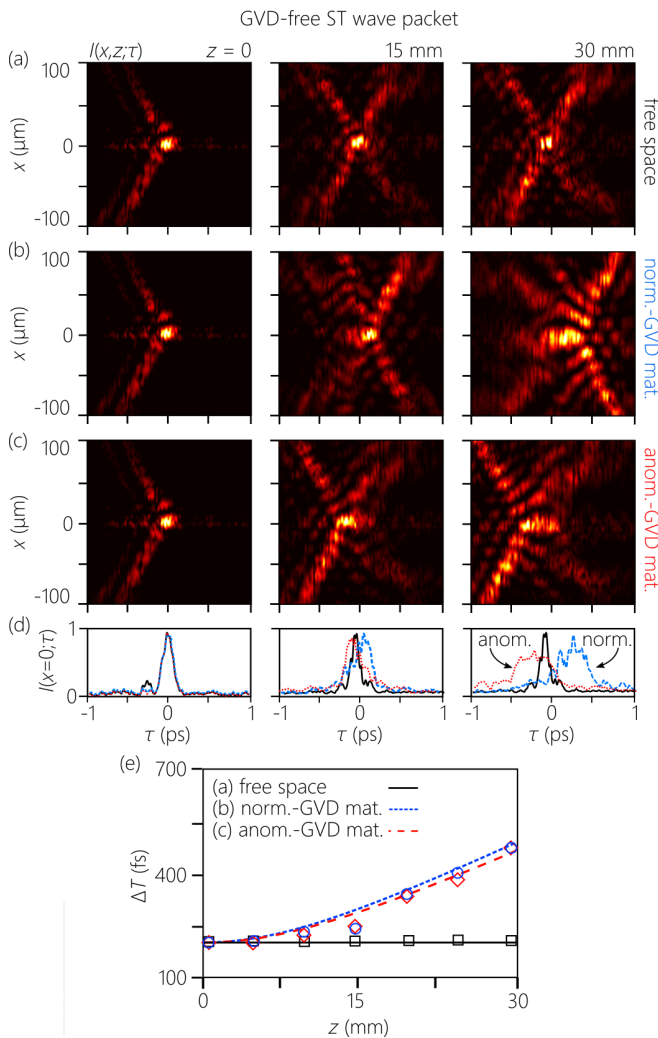


FIG. 6. (a-c) Measured spatio-temporal intensity profiles  $I(x, z; \tau)$  at  $z = 0, 15 \text{ mm},$  and  $30 \text{ mm}$  for a ST wave packet (a) in free space, (b) in a normal-GVD medium, and (c) in an anomalous-GVD medium. The ST wave packet is propagation invariant in free space (a), and thus experiences GVD in the dispersive media (b,c). (d) On-axis  $x = 0$  profiles  $I(0, z; \tau)$  for the ST wave packets in (a-c). The three panels provide the pulse profiles at  $z = 0$  (where all three coincide),  $z = 15 \text{ mm},$  and  $z = 30 \text{ mm}$  (where the pulses in the dispersive media have dispersed). (e) On-axis pulsewidth  $\Delta T$  measured at 5-mm axial intervals

whereas the pulsewidth in the medium is constant after GVD-cancellation [Fig. 7(g,h)].

### C. Independence of the group velocity and GVD-cancellation

The measurements in Fig. 7 were carried out at a fixed group velocity  $\tilde{v}_a$  in free space. In many nonlinear optical applications that benefit from GVD-cancellation, it is also useful to also control the wave-packet group velocity. This can help group-velocity matching between pulses at

disparate wavelengths while exploiting long crystals. In our scheme, the angular dispersion profile  $\varphi(\lambda)$  can be controlled almost arbitrarily [Fig. 4]: each wavelength  $\lambda$  can be assigned a propagation angle  $\varphi(\lambda)$  independently of all other wavelengths, and we can thus tune  $\tilde{v}_a$  and  $k_{2a}$  independently [60]. We demonstrate this capability in Fig. 8 where we measure the group delay in normal- and anomalous-GVD samples of *fixed* length ( $L = 30 \text{ mm}$ ) while varying the spectral tilt angle  $\theta_a$  in free space. This results in tuning of the free-space group velocity  $\tilde{v}_a = c \tan \theta_a$  and hence the group velocity  $\tilde{v}$  in the medium (Eq. 2). Throughout, we maintain GVD-cancellation; that is, the wave packet is invariant after the sample *independently* of  $\tilde{v}_a$ . As  $\tilde{v}_a$  is increased continuously from the subluminal regime ( $\theta_a < 45^\circ, \tilde{v}_a < c$ ) to the superluminal ( $\theta_a > 45^\circ, \tilde{v}_a > c$ ) regime, the group velocity of the wave packet in the medium  $\tilde{v}$  also increases, resulting in a concomitant drop in the group delay over the fixed sample length. This confirms that GVD-cancellation and group-velocity-tunability can be maintained independently of each other.

## VIII. INVERTING THE GROUP-VELOCITY DISPERSION

When GVD-cancellation is *not* achieved, the GVD coefficient in the medium  $k'_{2m}$  is given by:

$$k'_{2m} = k_{2m} + \frac{k_{2a}}{n_m} + \frac{1}{n_m} \frac{\Delta}{c\omega_o}. \quad (8)$$

In other words, the effective GVD in the medium  $k'_{2m}$  combines the intrinsic material GVD  $k_{2m}$  (due to chromatic dispersion) with the free-space GVD introduced into the ST wave packet (via non-differentiable angular dispersion), in addition to the negligible offset  $\Delta$ . By varying  $k_{2a}$  we can realize one of three different scenarios. First, the GVD introduced in free space can reinforce the GVD in the medium ( $k_{2a}$  has the same sign as  $k_{2m}$ ), leading to GVD *enhancement* ( $|k'_{2m}| > |k_{2m}|$ ). We present measurements for such a scenario in Fig. 9(a,d) where we enhance the dispersion in the normal-GVD medium by introducing normal-GVD in free space [Fig. 9(a)], and similarly enhance the dispersion in the anomalous-GVD regime by introducing anomalous GVD in free space [Fig. 9(d)]. Comparing Fig. 9(a,d) to Fig. 6(b,c) confirms the enhanced pulse broadening. Second, the GVD experienced by the wave packet in the medium can be *cancelled*  $k'_{2m} = 0$  by setting  $k_{2a} = -n_m k_{2m} - \frac{\Delta}{c\omega_o}$  [Fig. 9(b,e)], which is the scenario dealt with above in Fig. 7.

Third, the effective GVD experienced by the wave packet in the medium can be *inverted* as shown in Fig. 9(c,f). By GVD-inversion we mean that the effective GVD coefficient in the medium  $k'_{2m}$  has the opposite sign as that of the intrinsic chromatic dispersion in the medium  $k_{2m}$  (of course, the magnitudes need not be equal). In Fig. 9(c), the ST wave packet traveling in ZnSe in the normal-GVD regime instead encounters *anomalous*



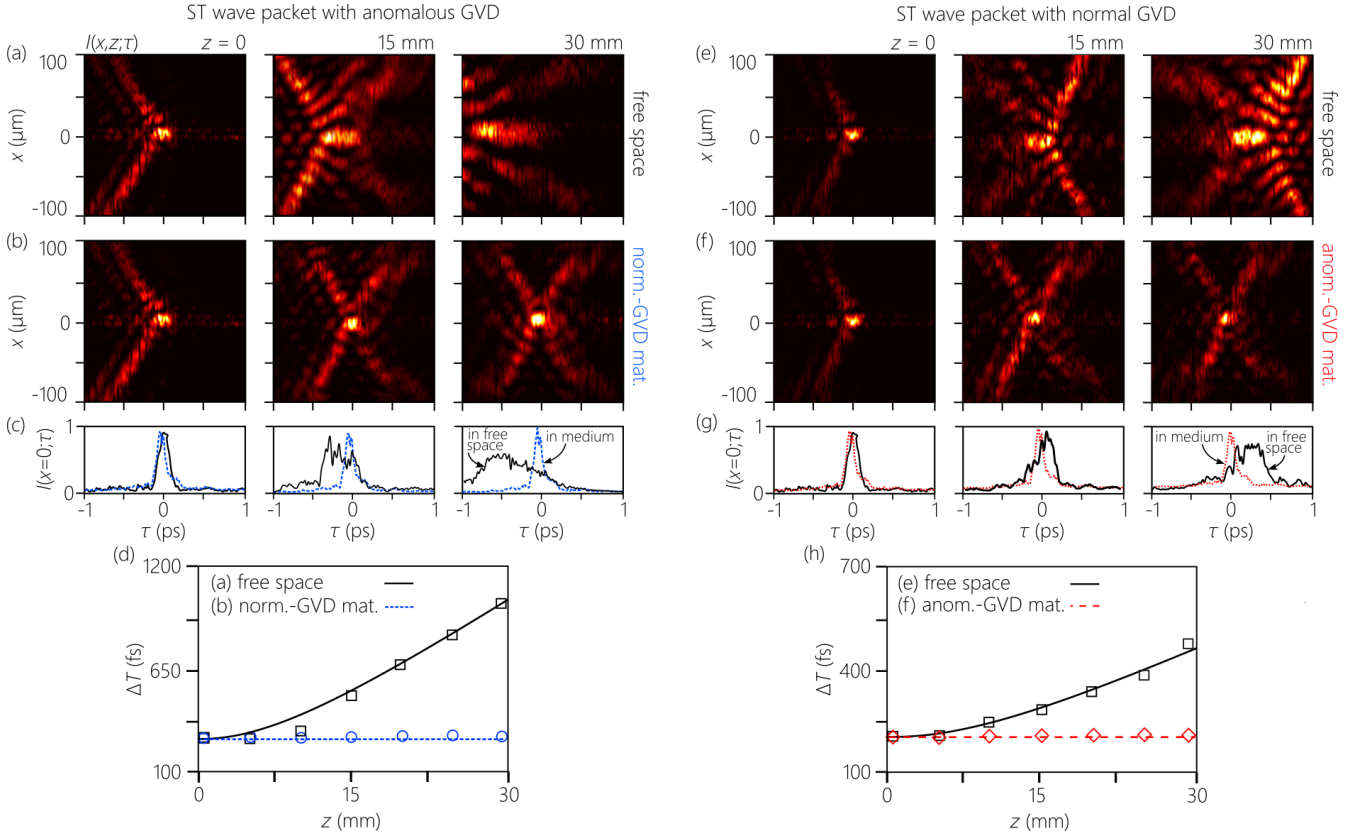


FIG. 7. Cancellation of either normal or anomalous GVD. (a) Measured spatio-temporal intensity profiles  $I(x, z; \tau)$  at  $z=0$ , 15 mm, and 30 mm for a ST wave packet endowed with anomalous GVD in free space, and (b) in a normal-GVD medium, whereupon dispersion is cancelled. (c) On-axis  $x=0$  profiles  $I(0, z; \tau)$  for the ST wave packets in (a,b). The panels provide the pulse profiles at  $z=0$  (where the two coincide),  $z=15$  mm, and  $z=30$  mm (where the pulse has dispersed in free space but not in the medium). (d) On-axis pulsewidth  $\Delta T$  measured at 5-mm axial intervals. (e) Measured spatio-temporal intensity profiles  $I(x, z; \tau)$  at  $z=0$ , 15 mm, and 30 mm for a ST wave packet endowed with normal GVD in free space, and (f) in an anomalous-GVD medium, whereupon dispersion is cancelled. (g,h) Same as (c,d) but for the ST wave packets in (e,f).

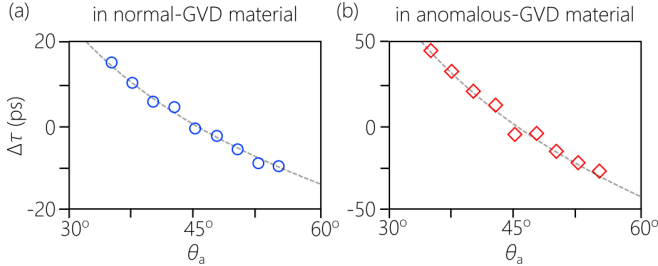


FIG. 8. (a) Measured group delay  $\Delta\tau$  for a ST wave packet with respect to a conventional pulsed plane-wave upon traversing a fixed-thickness medium ( $L=30$  mm) while tuning the free-space spectral tilt angle  $\theta_a$ . This wave packet is endowed with anomalous GVD in free space and is coupled to a normal-GVD medium where it is GVD-free. (b) Same as (a) but for a ST wave packet endowed with normal GVD in free space traversing a fixed-thickness medium having anomalous GVD. The dashed curves in (a,b) are the theoretical predictions  $\Delta\tau = \frac{L}{c} \tilde{n}$ , where  $\tilde{n}$  is determined from Eq. 2.

GVD. Here the anomalous GVD introduced in free space

overcomes the normal GVD in the medium and renders it effectively an anomalous-GVD medium. Similarly, the ST wave packet in Fig. 9(f) traveling in the anomalous-GVD medium encounters instead normal GVD. This can be useful in exploiting media that have desirable nonlinear coefficients for particular interactions but whose sign of GVD at the wavelength of interest is opposite of what is needed.

## IX. DISCUSSION AND CONCLUSION

We emphasize again the distinction between ‘dispersion compensation’ and ‘dispersion cancellation’. In the former, *after* a conventional pulse traverses a dispersive medium, an optical system compensates for the dispersion (in principle of any order or sign) encountered by removing the accumulated spectral phase. This can be accomplished using a  $4f$  spectral phase modulator [10] or other systems. By ‘dispersion cancellation’ we refer to modifying the structure of the optical field by introducing angular dispersion, such that it propagates invariantly

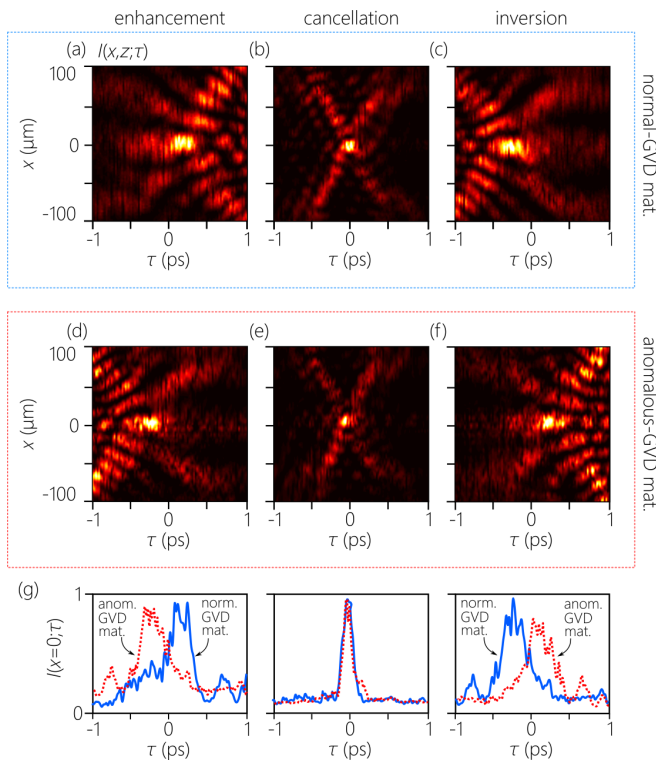


FIG. 9. Enhancing, eliminating, and inverting GVD in a dispersive medium by varying the GVD introduced into the ST wave packet in free space. (a-c) Spatio-temporal intensity profiles at  $z = 30$  mm in ZnSe (normal GVD) while varying the free-space GVD: (a)  $c\omega_0 k_{2a} = 0.8$ , (b)  $-0.8$ , and (c)  $-2.25$ . (d-f) Same as (a-c) but for the anomalous-GVD sample: (d)  $c\omega_0 k_{2a} \approx -0.25$ , (e)  $0.25$ , and (f)  $0.75$ . In (a,d) the GVD experienced by the ST wave packets is enhanced; in (b,e) the GVD is cancelled; and in (c,f) the GVD is inverted.

in the dispersive medium. Whereas conventional angular dispersion (in TPFs) can cancel normal GVD but *not* anomalous GVD, we have demonstrated here that non-differentiable angular dispersion (in ST wave packets) enables GVD-cancellation in both the normal and anomalous regimes.

Although the existence of propagation-invariant ST wave packets in presence of normal or anomalous GVD was known theoretically, the lack of experimental strategies for producing non-differentiable angular dispersion precluded putting these predictions to test in the linear regime. Another obstacle faced previously is that the required ST wave packets were of the ‘baseband’ class; i.e., their spatial spectra are centered at  $k_x = 0$  [64]. Until recently, all experimentally generated ST wave packets in free space were of the ‘sideband’ variety; i.e., their spatial spectra are centered at  $k_x \neq 0$  and the low spatial frequencies in the vicinity of  $k_x = 0$  are excluded on physical grounds [64]. Examples include focus-wave modes [68–70] and X-waves [71, 72]. Both of these obstacles are overcome by exploiting the universal angular dispersion synthesizer in [59]. Although such an approach intro-

duces arbitrary angular dispersion in one transverse dimension only, recent progress has extended this strategy to both transverse dimensions [73–75].

Although a previous experiment demonstrated normal-GVD cancellation in silica using modified X-waves [76, 77], no attempts at cancelling anomalous GVD by exploiting focus-wave modes, X-waves, or other sideband ST wave packets have been reported. Baseband ST wave packets have been synthesized via energy-inefficient spatio-temporal amplitude filtering for cancelling anomalous [78] and normal [79] GVD, but propagation invariance in presence of dispersion was not verified. Finally, theoretical studies have uncovered a host of structural field transitions for dispersion-free ST wave packets in dispersive media that have no analogs in free space, including a transition from X-shaped to O-shaped profiles while tuning the group velocity in presence of anomalous GVD [23], and even more complex transitions in the normal-GVD regime [22]. All such transitions occur at a *fixed* wavelength (in contrast to [80, 81] where the transition requires changing the GVD sign). None of these phenomena have been observed to date, and an O-shaped ST wave packet has not yet been reported. We anticipate that the work presented here can provide the platform for studying these structural dynamics in dispersive media.

In conclusion, we have realized – for the first time to the best of our knowledge – dispersion-free propagation in dispersive media symmetrically in the normal- and anomalous-GVD regimes. By incorporating non-differentiable angular dispersion into a pulsed field we produce ST wave packets whose group velocity and GVD coefficient can be tuned in free space independently of each other. We have confirmed dispersion-free propagation of 200-fs pulses at a wavelength  $\lambda_0 \approx 1 \mu\text{m}$  in ZnSe (normal GVD) and chirped Bragg mirrors (anomalous GVD). Moreover, because the GVD in the medium combines additively with the GVD introduced into the ST wave packet in free space, we have succeeded in demonstrating GVD-inversion: the wave packet experiences normal GVD while propagating in a medium in its anomalous-GVD regime, and vice versa. Moreover, we have demonstrated this unprecedented level of GVD control independently of the wave-packet group velocity, which can be tuned separately. These results are useful in multi-wavelength nonlinear interactions and quantum optics in long crystals.

#### APPENDIX: COUPLING A TILTED-PULSE FRONT TO A DISPERSIVE MEDIUM

In an on-axis TPF in free space, the propagation angle with respect to the  $z$ -axis takes the general form  $\varphi_a(\omega_0 + \Omega) \approx \varphi_a^{(1)}\Omega + \frac{1}{2}\varphi_a^{(2)}\Omega^2$ , with  $\varphi_a(\omega_0) = 0$ ,  $\varphi_a^{(n)} = \frac{d^n \varphi_a}{d\omega} \Big|_{\omega_0}$ , and we similarly expand  $k_x$  and  $k_z$ ,  $k_x(\omega) \approx k_x^{(0)} + k_x^{(1)}\Omega + \frac{1}{2}k_x^{(2)}\Omega^2$ , and  $k_z(\omega) \approx k_z^{(0)} + k_z^{(1)}\Omega + \frac{1}{2}k_z^{(2)}\Omega^2$ ; where  $k_x^{(0)} = 0$ ,  $ck_x^{(1)} = \omega_0 \varphi_a^{(1)}$ ,  $c\omega_0 k_x^{(2)} = 2\omega_0 \varphi_a^{(1)} + \omega_0^2 \varphi_a^{(2)}$ ,

$k_z^{(0)} = k_o$ ,  $ck_z^{(1)} = 1$ , and  $c\omega_o k_z^{(2)} = -(\omega_o \varphi_a^{(1)})^2$  [16]. The last equation indicates that only anomalous GVD can be produced in free space on-axis with conventional angular dispersion. In a dispersive medium, the expansion coefficients for  $k_x$  and  $k_z$  are:  $k_x^{(0)} = 0$ ,  $ck_x^{(1)} = n_m \omega_o \varphi_m^{(1)}$ ,  $c\omega_o k_x^{(2)} = 2\tilde{n}_m \omega_o \varphi_m^{(1)} + n_m \omega_o^2 \varphi_m^{(2)}$ ,  $k_z^{(0)} = n_m k_o$ ,  $ck_z^{(1)} = \tilde{n}_m$ , and  $c\omega_o k_z^{(2)} = c\omega_o k_2 - n_m (\omega_o \varphi_m^{(1)})^2$ .

Because  $k_x$  is invariant across a planar interface at normal incidence, matching the first-order expansion coefficients for  $k_x$  yields  $\varphi_a^{(1)} = n_m \varphi_m^{(1)}$ , which can be recognized as the law of refraction for TPFs at normal incidence. Dispersion-free propagation in the medium  $k_z^{(2)} = 0$  requires that  $\omega_o \varphi_a^{(1)} = \tan \delta_a^{(1)} = \sqrt{n_m c \omega_o k_{2m}}$ . Only normal GVD  $k_{2m} > 0$  can be cancelled. The corresponding TPF in free space has a GVD coefficient  $k_z^{(2)} = -n_m k_{2m}$ . Therefore, GVD-cancellation requires exercising control over only first-order angular dispersion. To simplify the synthesis of the TPF in free space, we set  $\varphi_a^{(n)} = 0$  for  $n \geq 2$ . This assumption does *not* lead to the elimination of  $\varphi_m^{(2)}$ , which is given by  $n_m \omega_o^2 \varphi_m^{(2)} = 2(1 - \frac{\tilde{n}_m}{n_m}) \omega_o \varphi_a^{(1)}$ . The transverse wave number is  $k_x(\omega) = \frac{\Omega}{\omega_o} \frac{\omega}{c} \tan \delta_a^{(1)}$ , which is differentiable with respect to  $\omega$  everywhere. In free space,  $k_x(\omega) = \frac{\omega}{c} \sin\{\varphi_a(\omega)\}$ , so that  $\varphi_a(\omega) \approx \frac{\Omega}{\omega_o} \tan \delta_a^{(1)}$ .

Although the TPF in the material is GVD-free, higher-order dispersion terms nevertheless exist because of the  $\varphi_m^{(2)}$  term. Of course one may eliminate the  $\varphi_m^{(2)}$  term by including an appropriate  $\varphi_a^{(2)}$  term in free space. However, this would add to the complexity of the system. Indeed, no known optical device – besides the universal angular-dispersion synthesizer [59] – has reported independent control over both  $\varphi_a^{(1)}$  and  $\varphi_a^{(2)}$ .

## ACKNOWLEDGMENTS

The authors acknowledge the support of the Office of Naval Research (ONR, Grant Nos. N00014-17-1-2458 and N00014-20-1-2789).

The authors declare no conflicts of interest.

## DATA AVAILABILITY

The data that support the findings of this study are available from the corresponding author upon reasonable request.

- 
- [1] B. E. A. Saleh and M. C. Teich, *Principles of Photonics* (Wiley, 2007).
  - [2] A. M. Weiner, *Ultrafast Optics* (John Wiley & Sons, Inc., 2009).
  - [3] D. Strickland and G. Mourou, Compression of amplified chirped optical pulses, *Opt. Commun.* **56**, 3219 (1985).
  - [4] R. L. Fork, O. E. Martinez, and J. P. Gordon, Negative dispersion using pairs of prisms, *Opt. Lett.* **9**, 150 (1984).
  - [5] O. E. Martinez, 3000 times grating compressor with positive group velocity dispersion: Application to fiber compensation in 1.3–1.6  $\mu\text{m}$  region, *IEEE J. Quantum Electron.* **23**, 59 (1987).
  - [6] W. E. White, F. G. Patterson, R. L. Combs, D. F. Price, and R. L. Shepherd, Compensation of higher-order frequency-dependent phase terms in chirped-pulse amplification systems, *Opt. Lett.* **18**, 1343 (1993).
  - [7] B. E. Lemoff and C. P. J. Barty, Quintic-phase-limited, spatially uniform expansion and recompression of ultrashort optical pulses, *Opt. Lett.* **18**, 1651 (1993).
  - [8] S. Kane and J. Squier, Grism-pair stretcher-compressor system for simultaneous second- and third-order dispersion compensation in chirped-pulse amplification, *J. Opt. Soc. Am. B* **14**, 661 (1997).
  - [9] S. Kane and J. Squier, Fourth-order-dispersion limitations of aberration-free chirped-pulse amplification systems, *J. Opt. Soc. Am. B* **14**, 1237 (1997).
  - [10] A. M. Weiner, Femtosecond pulse shaping using spatial light modulators, *Rev. Sci. Instrum.* **71**, 1929 (2000).
  - [11] A. F. J. Runge, D. D. Hudson, K. K. K. Tam, C. M. de Sterke, and A. Blanco-Redondo, The pure-quartic soliton laser, *Nat. Photon.* **14**, 492 (2020).
  - [12] J. P. Torres, M. Hendrych, and A. Valencia, Angular dispersion: an enabling tool in nonlinear and quantum optics, *Adv. Opt. Photon.* **2**, 319 (2010).
  - [13] S. Szatmári, P. Simon, and M. Feuerhake, Group-velocity-dispersion-compensated propagation of short pulses in dispersive media, *Opt. Lett.* **21**, 1156 (1996).
  - [14] J. A. Fülöp and J. Hebling, Applications of tilted-pulse-front excitation, in *Recent Optical and Photonic Technologies*, edited by K. Y. Kim (InTech, 2010).
  - [15] O. E. Martinez, J. P. Gordon, and R. L. Fork, Negative group-velocity dispersion using refraction, *J. Opt. Soc. Am. A* **1**, 1003 (1984).
  - [16] M. A. Porras, G. Valiulis, and P. Di Trapani, Unified description of Bessel X waves with cone dispersion and tilted pulses, *Phys. Rev. E* **68**, 016613 (2003).
  - [17] M. A. Porras, S. Trillo, C. Conti, and P. Di Trapani, Paraxial envelope X waves, *Opt. Lett.* **28**, 1090 (2003).
  - [18] S. Longhi, Localized subluminal envelope pulses in dispersive media, *Opt. Lett.* **29**, 147 (2004).
  - [19] M. A. Porras and P. Di Trapani, Localized and stationary light wave modes in dispersive media, *Phys. Rev. E* **69**, 066606 (2004).
  - [20] D. N. Christodoulides, N. K. Efremidis, P. Di Trapani, and B. A. Malomed, Bessel X waves in two- and three-dimensional bidispersive optical systems, *Opt. Lett.* **29**, 1446 (2004).
  - [21] M. S. Mills, G. A. Siviloglou, N. Efremidis, T. Graf, E. M. Wright, J. V. Moloney, and D. N. Christodoulides, Localized waves with spherical harmonic symmetries, *Phys. Rev. A* **86**, 063811 (2012).
  - [22] S. Malaguti and S. Trillo, Envelope localized waves of the conical type in linear normally dispersive media, *Phys.*

- Rev. A **79**, 063803 (2009).
- [23] S. Malaguti, G. Bellanca, and S. Trillo, Two-dimensional envelope localized waves in the anomalous dispersion regime, *Opt. Lett.* **33**, 1117 (2008).
- [24] P. Di Trapani, G. Valiulis, A. Piskarskas, O. Jedrkiewicz, J. Trull, C. Conti, and S. Trillo, Spontaneously generated X-shaped light bullets, *Phys. Rev. Lett.* **91**, 093904 (2003).
- [25] D. Faccio, M. A. Porras, A. Dubietis, F. Bragheri, A. Couairon, and P. Di Trapani, Conical emission, pulse splitting, and X-wave parametric amplification in nonlinear dynamics of ultrashort light pulses, *Phys. Rev. Lett.* **96**, 193901 (2006).
- [26] D. Faccio, A. Averchi, A. Couairon, M. Kolesik, J. Moloney, A. Dubietis, G. Tamosauskas, P. Polesana, A. Piskarskas, and P. D. Trapani, Spatio-temporal reshaping and X wave dynamics in optical filaments, *Opt. Express* **15**, 13077 (2007).
- [27] M. A. Porras, A. Dubietis, A. Matijošius, R. Piskarskas, F. Bragheri, A. Averchi, and P. Di Trapani, Characterization of conical emission of light filaments in media with anomalous dispersion, *J. Opt. Soc. Am. B* **24**, 581 (2007).
- [28] H. E. Kondakci and A. F. Abouraddy, Diffraction-free pulsed optical beams via space-time correlations, *Opt. Express* **24**, 28659 (2016).
- [29] K. J. Parker and M. A. Alonso, The longitudinal isophase condition and needle pulses, *Opt. Express* **24**, 28669 (2016).
- [30] M. A. Porras, Gaussian beams diffracting in time, *Opt. Lett.* **42**, 4679 (2017).
- [31] N. K. Efremidis, Spatiotemporal diffraction-free pulsed beams in free-space of the Airy and Bessel type, *Opt. Lett.* **42**, 5038 (2017).
- [32] M. A. Porras, Nature, diffraction-free propagation via space-time correlations, and nonlinear generation of time-diffracting light beams, *Phys. Rev. A* **97**, 063803 (2018).
- [33] M. Yessenov, B. Bhaduri, H. E. Kondakci, and A. F. Abouraddy, Weaving the rainbow: Space-time optical wave packets, *Opt. Photon. News* **30**, 34 (2019).
- [34] M. Yessenov, L. A. Hall, K. L. Schepler, and A. F. Abouraddy, Space-time wave packets, arXiv:2201.08297 (2022).
- [35] L. J. Wong and I. Kaminer, Ultrashort tilted-pulsefront pulses and nonparaxial tilted-phase-front beams, *ACS Photon.* **4**, 2257 (2017).
- [36] H. E. Kondakci and A. F. Abouraddy, Optical space-time wave packets of arbitrary group velocity in free space, *Nat. Commun.* **10**, 929 (2019).
- [37] M. Yessenov, B. Bhaduri, L. Mach, D. Mardani, H. E. Kondakci, M. A. Alonso, G. A. Atia, and A. F. Abouraddy, What is the maximum differential group delay achievable by a space-time wave packet in free space?, *Opt. Express* **27**, 12443 (2019).
- [38] M. Yessenov and A. F. Abouraddy, Changing the speed of coherence in free space, *Opt. Lett.* **44**, 5125 (2019).
- [39] H. E. Kondakci and A. F. Abouraddy, Self-healing of space-time light sheets, *Opt. Lett.* **43**, 3830 (2018).
- [40] B. Bhaduri, M. Yessenov, and A. F. Abouraddy, Anomalous refraction of optical spacetime wave packets, *Nat. Photon.* **14**, 416 (2020).
- [41] A. M. Allende Motz, M. Yessenov, and A. F. Abouraddy, Isochronous space-time wave packets, *Opt. Lett.* **46**, 2260 (2021).
- [42] M. Yessenov, B. Bhaduri, and A. F. Abouraddy, Refraction of space-time wave packets: I. Theoretical principles, arXiv:2104.12965 (2021).
- [43] A. M. Allende Motz, M. Yessenov, B. Bhaduri, and A. F. Abouraddy, Refraction of optical space-time wave packets: II. Experiments at normal incidence, arXiv:2104.12969 (2021).
- [44] M. Yessenov, A. M. Allende Motz, B. Bhaduri, and A. F. Abouraddy, Refraction of optical space-time wave packets: III. Experiments at oblique incidence, arXiv:2104.12972 (2021).
- [45] L. A. Hall, M. Yessenov, S. A. Ponomarenko, and A. F. Abouraddy, The space-time Talbot effect, *APL Photon.* **6**, 056105 (2021).
- [46] H. E. Kondakci, M. A. Alonso, and A. F. Abouraddy, Classical entanglement underpins the propagation invariance of space-time wave packets, *Opt. Lett.* **44**, 2645 (2019).
- [47] B. Bhaduri, M. Yessenov, D. Reyes, J. Pena, M. Meem, S. R. Fairchild, R. Menon, M. C. Richardson, and A. F. Abouraddy, Broadband space-time wave packets propagating 70 m, *Opt. Lett.* **44**, 2073 (2019).
- [48] M. Yessenov, B. Bhaduri, P. J. Delfyett, and A. F. Abouraddy, Free-space optical delay line using space-time wave packets, *Nat. Commun.* **11**, 5782 (2020).
- [49] A. Shiri, M. Yessenov, S. Webster, K. L. Schepler, and A. F. Abouraddy, Hybrid guided space-time optical modes in unpatterned films, *Nat. Commun.* **11**, 6273 (2020).
- [50] K. L. Schepler, M. Yessenov, Y. Zhiyenbayev, and A. F. Abouraddy, Space-time surface plasmon polaritons: A new propagation-invariant surface wave packet, *ACS Photon.* **7**, 2966 (2020).
- [51] A. Shiri, M. Yessenov, R. Aravindakshan, and A. F. Abouraddy, Omni-resonant space-time wave packets, *Opt. Lett.* **45**, 1774 (2020).
- [52] B. Kibler and P. Béjot, Discretized conical waves in multimode optical fibers, *Phys. Rev. Lett.* **126**, 023902 (2021).
- [53] P. Béjot and B. Kibler, Spatiotemporal helicon wavepackets, *ACS Photon.* **8**, 2345 (2021).
- [54] P. N. Ruano, C. W. Robson, and M. Ornigotti, Localized waves carrying orbital angular momentum in optical fibers, *J. Opt.* **23**, 075603 (2021).
- [55] C. Guo and S. Fan, Generation of guided space-time wave packets using multilevel indirect photonic transitions in integrated photonics, *Phys. Rev. Research* **3**, 033161 (2021).
- [56] L. A. Hall, M. Yessenov, and A. F. Abouraddy, Space-time wave packets violate the universal relationship between angular dispersion and pulse-front tilt, *Opt. Lett.* **46**, 1672 (2021).
- [57] L. A. Hall and A. F. Abouraddy, Realizing normal group-velocity dispersion in free space via angular dispersion, *Opt. Lett.* **46**, 5421 (2021).
- [58] L. A. Hall and A. F. Abouraddy, Consequences of non-differentiable angular dispersion in optics: Tilted pulse fronts versus space-time wave packets, arXiv:2109.07039 (2021).
- [59] L. A. Hall and A. F. Abouraddy, A universal angular-dispersion synthesizer, arXiv:2109.13987 (2021).
- [60] M. Yessenov, L. A. Hall, and A. F. Abouraddy, Engineering the optical vacuum: Arbitrary magnitude, sign, and order of dispersion in free space using space-time wave

- packets, *ACS Photonics* **8**, 2274 (2021).
- [61] J. P. Gordon and R. L. Fork, Optical resonator with negative dispersion, *Opt. Lett.* **9**, 153 (1984).
- [62] R. Donnelly and R. Ziolkowski, Designing localized waves, *Proc. R. Soc. Lond. A* **440**, 541 (1993).
- [63] H. E. Kondakci and A. F. Abouraddy, Diffraction-free space-time beams, *Nat. Photon.* **11**, 733 (2017).
- [64] M. Yessenov, B. Bhaduri, H. E. Kondakci, and A. F. Abouraddy, Classification of propagation-invariant space-time light-sheets in free space: Theory and experiments, *Phys. Rev. A* **99**, 023856 (2019).
- [65] H. He, C. Guo, and M. Xiao, Non-dispersive space-time wave packets propagating in dispersive media, *arXiv:2109.00782* (2021).
- [66] M. Yessenov, S. Faryadras, S. Benis, D. J. Hagan, E. W. Van Stryland, and A. F. Abouraddy, Refraction of space-time wave packets in a dispersive medium, *arXiv:2112.04003* (2021).
- [67] D. T. F. Marple, Refractive index of ZnSe, ZnTe, and CdTe, *J. Appl. Phys.* **35**, 539 (1964).
- [68] J. N. Brittingham, Focus wave modes in homogeneous Maxwell's equations: Transverse electric mode, *J. Appl. Phys.* **54**, 1179 (1983).
- [69] K. Reivelt and P. Saari, Optical generation of focus wave modes, *J. Opt. Soc. Am. A* **17**, 1785 (2000).
- [70] K. Reivelt and P. Saari, Experimental demonstration of realizability of optical focus wave modes, *Phys. Rev. E* **66**, 056611 (2002).
- [71] J.-Y. Lu and J. F. Greenleaf, Nondiffracting X waves – exact solutions to free-space scalar wave equation and their finite aperture realizations, *IEEE Trans. Ultrason. Ferroelec. Freq. Control* **39**, 19 (1992).
- [72] P. Saari and K. Reivelt, Evidence of X-shaped propagation-invariant localized light waves, *Phys. Rev. Lett.* **79**, 4135 (1997).
- [73] C. Guo, M. Xiao, M. Orenstein, and S. Fan, Structured 3D linear space-time light bullets by nonlocal nanophotonics, *Light Sci. Appl.* **10**, 160 (2021).
- [74] K. Pang, K. Zou, H. Song, Z. Zhao, A. Minoofar, R. Zhang, H. Song, H. Zhou, X. Su, C. Liu, N. Hu, M. Tur, and A. E. Willner, Simulation of near-diffraction- and near-dispersion-free oam pulses with controllable group velocity by combining multiple frequencies, each carrying a bessel mode, *Opt. Lett.* **46**, 4678 (2021).
- [75] M. Yessenov, J. Free, Z. Chen, E. G. Johnson, M. P. J. Lavery, M. A. Alonso, and A. F. Abouraddy, Space-time wave packets localized in all dimensions, *arXiv:2111.03095* (2021).
- [76] H. Sönajalg and P. Saari, Suppression of temporal spread of ultrashort pulses in dispersive media by bessel beam generators, *Opt. Lett.* **21**, 1162 (1996).
- [77] H. Sönajalg, M. Rätsep, and P. Saari, Demonstration of the Bessel-X pulse propagating with strong lateral and longitudinal localization in a dispersive medium, *Opt. Lett.* **22**, 310 (1997).
- [78] M. Dallaire, N. McCarthy, and M. Piché, Spatiotemporal bessel beams: theory and experiments, *Opt. Express* **17**, 18148 (2009).
- [79] O. Jedrkiewicz, Y.-D. Wang, G. Valiulis, and P. Di Trapani, One dimensional spatial localization of polychromatic stationary wave-packets in normally dispersive media, *Opt. Express* **21**, 25000 (2013).
- [80] M. A. Porras, A. Dubietis, E. Kučinskas, F. Bragheri, V. Degiorgio, A. Couairon, D. Faccio, and P. Di Trapani, From X- to O-shaped spatiotemporal spectra of light filaments in water, *Opt. Lett.* **30**, 3398 (2005).
- [81] N. A. Panov, D. E. Shipilo, I. A. Nikolaeva, V. O. Kompanets, S. V. Chekalin, and O. G. Kosareva, Continuous transition from X- to O-shaped angle-wavelength spectra of a femtosecond filament in a gas mixture, *Phys. Rev. A* **103**, L021501 (2021).